Table 1 Baseline of hepatitis C virus patients with normal serum aminotransferase (ALT) received antiviral therapy

	ALT ≤ 30 U/L (group A)	ALT 31–40 U/L (group B)	*P*-value
No. patients	255	209	
Age	51.6 ± 13.0	53.5 ± 13.2	0.548*
Sex (male/female)	112/143	117/92	0.01**
BMI (kg/m^2)	21.6 ± 2.9	22.8 ± 3.0	<0.001*
HOMA-IR	2.5 ± 3.2	5.2 ± 6.5	0.093*
Genotype: 1/2/others	127/127/1	112/96/1	0.881**
Viral load: low/high	138/117	99/110	0.203**
G1 (low/high)	114/125		
G2 (low/high)	161/62		
Histology			
F stage (0/1/2/3/4)	29/166/48/11/1	22/122/57/6/2	0.169**
Grade (0/1/2/3)	25/187/41/2	7/159/43/0	0.046**
Fatty change† 0–1/2–4	232/23	161/48	0.033**
Iron load‡ 0/1–4	101/15	97/19	0.458**
Ferritin (ng/mL)	83.9 ± 103.7	118.8 ± 135.3	0.006*
PLT count (/μL)	19.2 ± 5.4	18.4 ± 6.1	0.059*
≥150 000/<150 000	204/51	141/68	0.002**
Hyaluronate (ng/mL)	60.8 ± 73.7	69.1 ± 73.0	0.249*
Duration of antiviral therapy (weeks)	25.6 ± 12.0	26.1 ± 12.1	0.297*
Effects of therapy			
SVR/non-SVR	142/113	99/110	0.075**

**P*-values were calculated by Mann–Whitney-*U*-test. ***Fisher-exact-test. †0: no fatty change, 1: ≤10%, 2: 11–33%, 3: 34–66%, 4: ≥67% of hepatocyte; ‡no stain by 400×, 1: few stains by 250×, 2: stains by 100×, 3: stains by 25×, 4: stains by 10×. There were significant differences in sex distribution ($P = 0.01$), BMI ($P = 0.01$), frequency of steatosis ($P = 0.033$), serum ferritin level ($P = 0.006$), grade of hepatic inflammation ($P = 0.046$), incidence of fatty change ($P = 0.033$), serum ferritin level ($P = 0.006$), and the incidence of low PLT counts ($P = 0.002$) between groups A and B. Values are expressed as mean ± SD.

ALT, alanine aminotransferase; BMI, body mass index; HOMA-IR, homeostasis model assessment-insulin resistance; PLT, platelet; SVR, sustained viral responders.

duration of therapy between 1995 and 2003 was 26 weeks for IFN monotherapy and 24 weeks for IFN/Riba combination therapy. In principle, 6–10 MU IFN was administered daily for 2 weeks and three times per week subsequently. The daily dosage of ribavirin was 600–1000 mg depending on body weight. Sustained viral responders (SVR) were defined as patients who were negative for serum HCV RNA 6 months after the completion of antiviral therapy.

All of the patients were divided into two groups (group A: ALT ≤ 30 U/L, group B: 31 U/L ≤ ALT ≤ 40 U/L) which were further divided into two subgroups based on PLT counts: group A-1 and B-1 (PLT counts ≥150 000/μL) and groups A-2 and B-2 (PLT counts <150 000/μL).

One hundred and twenty-nine HCV carriers with PNALT were enrolled to determine their long-term prognosis. These patients showed normal serum ALT levels (≤30 U/L) over a 12-month period on least three different occasions (PLT counts ≥150 000/μL, and body mass index [BMI] <25 kg/m^2). Thirty-nine patients received serial liver biopsies. The mean follow-up period of the 129 patients was 7.2 ± 3.2 years on 15 November 2006.

Statistical analyses

Data are expressed as mean ± SD. We compared continuous variables using the Mann–Whitney *U*-test. A frequency analysis and comparison between the groups were performed using the χ^2-test or Fisher's exact test and the Mann–Whitney *U*-test. ANOVA and Tukey's HSD procedure was used to determine the difference between multiple groups. All tests were two-tailed and *P*-values of less than 0.05 were considered significant. All statistical analyses were performed using Statistical Package of Services Solutions software, version 11.0 (SPSS, Chicago, IL, USA).

Table 2 Baseline of hepatitis C virus patients with less than 30 U/L aminotransferase who received antiviral therapy

	PLT ≥ 150 000/mL (group A-1)	PLT < 150 000/mL (group A-2)	*P*-value
No. patients	204	51	
Age	48.4 ± 12.7	58.7 ± 7.5	<0.001*
Sex (male/female)	90/114	22/29	1.000**
BMI (kg/m^2)	21.6 ± 3.0	21.3 ± 2.4	0.514*
HOMA-IR	2.8 ± 3.5	1.2 ± 0.8	0.598*
Genotype: 1/2/others	101/101/2	25/26/0	0.952**
Viral load: low/high	112/92	26/25	0.574**
Histology			
F stage (0/1/2/3/4)	29/142/27/6/0	1/25/21/3/1	<0.001**
Grade (0–1/2,3)	179/25	33/18	<0.001**
Fatty change† 0–1/2–4	188/16	44/7	0.582**
Iron load‡ 0/1–4	82/12	17/3	0.762**
Ferritin (ng/mL)	86.0 ± 112.1	73.9 ± 46.6	0.204*
PLT count (/μL)	21.0 ± 4.4	12.1 ± 2.5	<0.001*
Hyaluronate (ng/mL)	41.8 ± 56.1	112.5 ± 109.9	<0.001*
Duration of antiviral therapy (weeks)	25.7 ± 10.3	27.0 ± 9.9	0.503*
Effects of therapy			
SVR/non-SVR	115/89	27/24	0.66**

**P*-values were calculated by Mann–Whitney-*U*-test. ***Fisher-exact-test. †0: no fatty change, 1: ≤10%, 2: 11–33%, 3: 34–66%, 4: ≥67% of hepatocyte; ‡no stain by 400×, 1: few stains by 250×, 2: stains by 100×, 3: stains by 25×, 4: stains by 10×. There were significant differences in age ($P < 0.001$), distribution of F stage ($P < 0.001$), grade of inflammatory activity ($P < 0.001$), PLT count ($P < 0.001$), and serum-hyaluronic acid ($P < 0.001$) between groups A-1 and A-2. Frequency of F2–4 patients was 16.2% in group A-1 and 51.6% in group A-2. Values are expressed as mean ± SD.

BMI, body mass index; HOMA-IR, homeostasis model assessment–insulin resistance; PLT, platelet counts; SVR, sustained viral responders.

RESULTS

Demographic, clinical, and histological features of 464 HCV carriers with normal serum ALT

THE CHARACTERISTICS OF the 464 HCV carriers with normal serum ALT are shown in Table 1. There were significant differences in sex, frequency of steatosis, serum ferritin levels, BMI, and the incidence of low PLT counts (<150 000/μL) between groups A and B.

There were significant differences in age, fibrosis (F) stage, inflammatory activity, PLT counts, and serum hyaluronate between groups A-1 and A-2 (Table 2). The frequency of stage F2–4 patients was 16.2% in group A-1, and 49.0% in group A-2 (Table 2). In group B, there were significant differences in age, F stage, PLT counts, and serum hyaluronate between groups B-1 and B-2 (Table 3). There were no F4 patients in group A-1 and B-1, and the frequency of F3 patients was very low compared with those in groups A-2 and B-2 (2.6% *vs* 7.6%). The PLT counts decreased in proportion to the progression of liver fibrosis as follows; F0 ($n = 51$); $20.7 \pm 5.2 \times 10^4$/μL, F1 ($n = 288$); $19.8 \pm 5.6 \times 10^4$/μL, F2 ($n = 105$); $16.9 \pm 5.3 \times 10^4$/μL, F3 ($n = 17$); $15.9 \pm 4.6 \times 10^4$/μL, and F4 ($n = 3$); $11.3 \pm 3.8 \times 10^4$/μL.

Of the 464 patients, the frequency of the F0–1 stages was 80.1% and that of the F2–4 stages was 19.9% in patients with PLT counts ≥150 000/μL, and it was 50.4% and 49.6%, respectively, in patients with PLT counts <150 000/μL. In patients with PLT counts $\geq 17.0 \times 10^4$/μL, 80.8% were in stages F0–1 and 19.2% were in stages F2–4, and in patients with PLT counts $< 17.0 \times 10^4$/μL, 60.1% were in stages F0–1 and 39.9% were in stages F2–4.

The SVR rates of IFN therapy were 52.4% in F0–1 patients, 49.5% in F2–4 patients ($P = 0.896$ by Fisher's exact test), and 58.0% and 43.8% ($P = 0.592$) in IFN/Riba therapy, respectively.

In patients with genotype 1b and high viral load, the SVR rate was 12.5%. The SVR rate in genotype 2 patients was 60.4% in the IFN group and 67.7% in the IFN/Riba combination therapy group.

Table 3 Baseline of hepatitis C virus carriers with 31–40 U/L aminotransferase who received antiviral therapy

	PLT ≥ 150 000/mL (group B-1)	PLT < 150 000/mL (group B-2)	*P*-value
No. patients	141	68	
Age	48.2 ± 11.9	57.9 ± 7.5	<0.001*
Sex (male/female)	80/61	37/31	0.751**
BMI (kg/m^2)	22.9 ± 3.1	22.7 ± 2.6	0.08*
HOMA-IR	3.0 ± 2.0	8.2 ± 9.5	0.8.8*
Genotype: 1/2/others	82/58/1	30/38/0	0.095**
Viral load: low/high	64/77	35/33	0.542**
Histology			
F stage (0/1/2/3/4)	17/91/31/2/0	4/30/26/6/2	<0.001**
Grade (0–1/2,3)	116/25	50/18	0.114**
Fatty change† 0–1/2–4	111/30	50/18	0.10**
Iron load‡ 0/1–4	67/12	30/7	0.762**
Ferritin (ng/mL)	114.4 ± 116.1	127.2 ± 167.8	0.869*
PLT count (/μL)	21.5 ± 4.9	12.2 ± 2.1	<0.001*
Hyaluronate (ng/mL)	46.9 ± 35.4	100.7 ± 0.98.1	<0.001*
Administration of IFN (weeks)	26.1 ± 11.9	27.7 ± 11.4	0.983*
Effects of therapy			
SVR/non-SVR	64/77	35/33	0.409**

**P*-values were calculated by Mann–Whitney-*U*-test. ***Fisher-exact-test. †0: no fatty change, 1: ≤10%, 2: 11–33%, 3: 34–66%, 4: ≥67% of hepatocyte; ‡no stain by 400×, 1: few stains by 250×, 2: stains by 100×, 3: stains by 25×, 4: stains by 10×. In group B, there were significant differences in age ($P < 0.001$), distribution of F stage ($P < 0.001$), PLT count ($P < 0.001$), and hyaluronic acid ($P < 0.001$) between B-1 and B-2. Frequency of F2–4 was 23.4% in B-1and 50.0% in B-2, respectively. Values are expressed as mean ± SD.
BMI, body mass index; HOMA-IR, homeostasis model assessment-insulin resistance; IFN, interferon; PLT, platelet counts; SVR, sustained viral responders.

Demographic, clinical, and histological features of 129 HCV carriers with PNALT

The demographic and clinical features of the 129 HCV carriers with PNALT who were followed up for 7.2 years are shown in Table 4. Normal liver histology was noted in 17 patients, 102 showed minimal to mild CH, and 10 had moderate CH. Steatosis was seen in 7% and iron loading was noted in 12%.[16]

Of the 78 patients followed longer than 7 years (mean follow-up period; 10.4 ± 3.1 years), 11 (14%) had continuously normal ALT (G-1), 43 (55%) showed a transient elevation of ALT (G-2), and 24 (31%) changed to CH with continuously elevated ALT (G-3).

Thirty-nine patients received repeated liver biopsies (2–4 times). Of the 39 patients, six were in G-1, 17 were in G-2, and 16 were in G-3. The intervals between the first biopsy and the last biopsy in these three groups were 7.1, 7.8, and 7.2 years, respectively. The progression of the F stage was noted in two of six in G-1, six of 17 in G-2, and seven of 16 in G-3. The median rates of fibrosis progression per year for these three groups were 0.05, 0.05, and 0.08 fibrosis unit. HCC was not detected in any patients during the follow-up periods.

Guidelines for the antiviral therapy of HCV carriers with normal serum ALT focused on the inhibition of the development of HCC

Considering the risk of progression to liver cirrhosis and the development of HCC, as well as the expected efficacy and various side-effects of antiviral therapy, an algorithm is needed for the management of HCV carriers with normal serum ALT. The progression rate of liver fibrosis stage was 0.05/year in HCV carriers with PNALT. The annual incidence of HCC in CH-C patients has been reported to be 0.5% at stages F0–F1, 1–2% at stage F2, 3–5% at stage F3, and 7% at stage F4.[4]

In principle, follow up without antiviral treatment is recommended for HCV carriers with PNALT (ALT ≤30 U/L) and PLT counts ≥150 000/μL, particularly in older patients (i.e. >65 years old), because over 90% show normal or minimal liver damage with good prognoses. However, antiviral therapy is not contraindicated for such patients since roughly 40% are infected with HCV genotype 2,[18] which suggests a high rate of SVR to the therapy with PEG-IFN/Riba.

As for the indication of antiviral therapy for HCV carriers with normal serum ALT (≤40 U/L), the PLT

Table 4 Characteristics of 129 HCV carriers with persistently normal ALT who received liver biopsy

	$n = 129$	Follow up over 5 years ($n = 78$)
Follow-up period (years)	7.2 ± 3.2	10.4 ± 3.1
Age (years)	48 (21–77)	45 (29–71)
Male ($n = 24$)	49.8 ± 16.4	42.3 ± 14.9
Female ($n = 105$)	47.2 ± 12.5	46.6 ± 11.6
Sex (male/female)	24/105	10/68
ALT (U/L)	8–30	9–30
Male ($n = 24$)	22.5 ± 5.7	21.1 ± 5.4
Female ($n = 105$)	21.6 ± 4.8	22.3 ± 5.1
PLT ($\times 10^4$/mL)	15–31	15–31
Ferritin (ng/mL)	5–225	5–225
Male ($n = 24$)	76.2 ± 53.5	84.6 ± 59.2
Female ($n = 105$)	60.0 ± 43.3	66.6 ± 52.5
HCV genotype	G1 ($n = 58$), G2 ($n = 45$) Mixed and unclassified ($n = 16$)	
BMI (kg/m^2)	16–27	16–27
Male	22.2 ± 1.7	21.9 ± 1.9
Female	21.3 ± 2.2	21.0 ± 2.4

Values are expressed as mean ± SD.
ALT, alanine aminotransferase; BMI, body mass index; HCV, hepatitis C virus; PLT, platelet.

count is a good indicator for discriminating as to whether or not they have minimal to mild fibrosis or moderate to advanced fibrosis. Serum hyaluronate levels were significantly higher in HCV carriers with 31–40 U/L ALT having less than 150 000/μL PLT (Table 3). Advanced hepatic F stage, an elevated ALT level, old age (>65 years old), and sex (male) are important risk factors for the development of HCC.[6,18,30] We advocated an algorithm for such patients (Fig. 1) taking into consideration the risk of the progression to cirrhosis and the development of HCC. Therapy with PEG-IFN/Riba is the first-line treatment; therapy for 48 weeks is recommended for genotype 1 patients with high viral load and 12–24 weeks therapy for genotypes 2 and 1 with low viral load.

DISCUSSION

OUR PREVIOUS STUDY in 129 HCV carriers with PNALT demonstrated a predominance of females, higher frequency of genotype 2, minimal to mild liver histology, and very slow progression of hepatic fibrosis.[18] However, over 30% of these patients advanced to CH-C with elevated ALT levels during the 7-year follow up.

There are many reports concerning the natural course of liver fibrosis in CH-C patients, including those who are HCV carriers with normal serum ALT.[19,31–39] More than half of CH-C patients show progression of F stage from F1 to F2–4 within 10 years, and it was reported that the progression of liver fibrosis in HCV carriers with normal serum ALT was more rapid than was observed in the present study.[23] The main reason for the discrepancy between the report by Puoti *et al.*[23] and our results might be due to the definitions used for the normal range of serum ALT. In our previous study, the patients were HCV carriers with PNALT (ALT ≤ 30 U/L) and PLT counts ≥150 000/μL. On the other hand, the patients in the study by Puoti *et al.* had ALT levels ≤40 U/L, irrespective of PLT counts, in which cirrhotic patients might be included.[23] However, recent studies have demonstrated that normal ALT levels are less than 30 U/L[24] or 25 U/L in men[40] and less than 19 U/L[24] or 22 U/L in women.[40]

The present study demonstrated that the different distribution of hepatic F stage became remarkable when the A and B groups were divided into two subgroups according to their PLT counts. In HCV carriers with ALT levels ≤30 U/L, the frequency of stages F2–3 was 16.2% among those with PLT counts ≥150 000/μL; however, the frequency of stages F2–3 was 49.0% in those with PLT counts <150 000/μL. Conversely, in HCV carriers with ALT levels between 31 and 40 U/L, the frequency of stages F2–4 was 23.4% among those with PLT counts ≥150 000/μL and 50.0% in those with PLT counts <150 000/μL. The PLT count is a useful marker in dis-

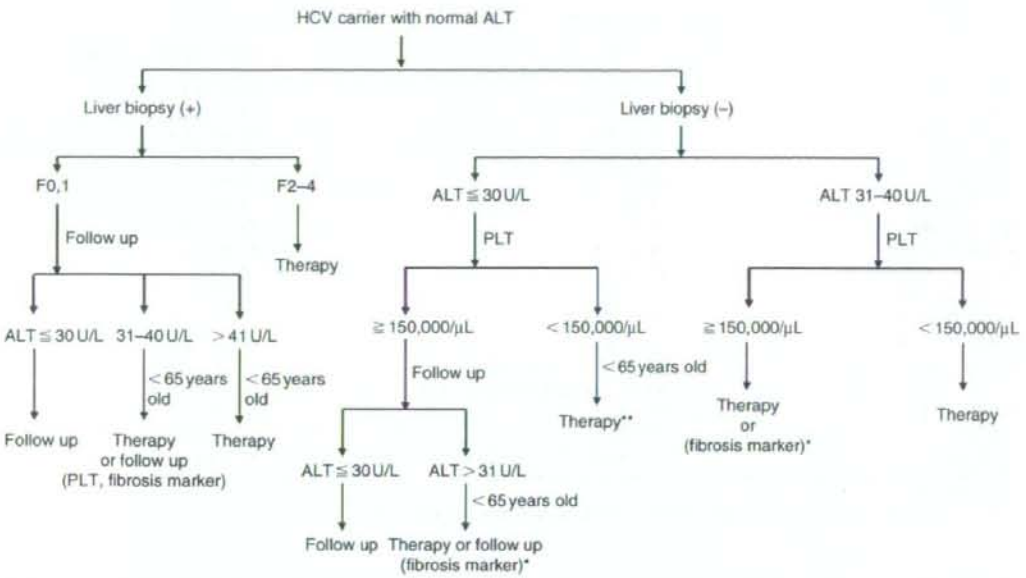

Figure 1 Algorithm for the management of hepatitis C virus (HCV) carriers with normal serum aminotransferase (ALT, ≤40 U/L) focused on the inhibition of the development of hepatocellular carcinoma. In patients who underwent liver biopsy, F0 and F1 patients younger than 65 years are candidates for antiviral therapy, especially those with genotype 2 after the elevation of serum ALT levels. In patients who did not undergo liver biopsy, ALT and platelet (PLT) levels are good indicators for determining candidates for antiviral therapy. Older patients (>65 years) and/or patients having uncontrolled hypertension, diabetes mellitus, or anemia should not be treated with pegylated interferon and ribavirin. Combination therapy with pegylated interferon and ribavirin for 48 weeks is recommended for patients with genotype 1 and high viral load, and 12–24 weeks therapy is suggested for patients with genotype 2 and genotype 1 with low viral load. *,**Serum fibrosis markers, such as hyaluronate, might be useful to decide whether patients are candidates for antiviral therapy or not.

criminating between stages F0–1 and F2–4 F in HCV carriers with normal serum ALT (≤40 U/L). In the present study, the mean PLT count in F2 and F3 patients was 16.9 ± 5.3 ($\times 10^4/\mu L$) and 15.9 ± 4.6 ($\times 10^4/\mu L$), respectively. The distribution of the F stage was not significantly different between patients with PLT counts $\geq 15 \times 10^4/\mu L$ versus $< 15 \times 10^4/\mu L$ and $\geq 17 \times 10^4/\mu L$ versus $< 17 \times 10^4/\mu L$.

The SVR rate for genotype 1 patients with high viral load treated with either IFN monotherapy or IFN/Riba were 12.5% and 37.7%, respectively. In genotype 2 patients with high viral load, the SVR rate in the present study was better than the data of Japanese CH-C patients with elevated ALT levels in our previous paper.[6] It was not reasonable to compare the SVR rates between HCV carriers with normal serum ALT and CH-C with elevated ALT in the present study, because the total dosage of IFN and the duration of treatment were significantly different.

The annual incidence of HCC is correlated with the progression of liver fibrosis, that is, the stage of liver disease.[2–4,6] Sustained low serum ALT levels are also associated with a lower incidence of HCC.[2,6,41] PEG-IFN/Riba therapy is expensive and induces various side-effects. The present results indicate that most HCV carriers with normal serum ALT (≤40 U/L) and PLT counts ≥150 000/μL have minimal to mild liver damage, indicating a low risk for the progression to cirrhosis and the development of HCC. This was more remarkable in patients with ALT levels ≤30 U/L and PLT counts ≥150 000/μL. However, nearly half of the patients with PLT count <150 000/μL have F2 or F3 F stages, indicating a certain risk for the progression to cirrhosis and the development of HCC. Fibrosis

progression is associated with age, baseline and follow-up ALT levels, inflammatory activity and steatosis in the initial liver biopsy, and alcohol consumption.[42] The present results indicate that most HCV carriers with PNALT have a good prognosis and a low risk of developing HCC.

Liver biopsy is a useful procedure for identifying the stage of liver fibrosis; however, it is invasive and may sometimes cause complications.[43,44] The error rate of predicting the F stage with this procedure can be estimated to be as high as 20%.[45] Recently introduced biochemical markers, such as FibroTest,[46] and FibroScan,[47–49] are excellent procedures for identifying liver fibrosis stage in CH-C patients.[50] The combined use of FibroScan and FibroTest is useful for accurately estimating moderate to severe liver fibrosis in most patients with CH-C, but not in F0 and F1 patients.[51]

Recently, Alberti proposed an individualized management algorithm for HCV carriers with PNALT with or without liver biopsy in which HCV genotype, patient age, motivation to receive antiviral therapy, and factors influencing side-effects were included.[52] The algorithm using a combination of serum ALT levels and PLT counts in the present study is simple, but it is useful because it focuses mainly on the inhibition of the progression to cirrhosis and the development of HCC.

ACKNOWLEDGMENTS

THIS PROJECT WAS supported in part by a grant-in-aid from the Ministry of Health, Labour and Welfare of Japan. Twelve hepatologists were from the Japanese Study Group of the Standard Antiviral Therapy for Viral Hepatitis (chief: Hiromitsu Kumada, Toranomon Hospital).

REFERENCES

1 Kasahara A, Hayashi N, Mochizuki K *et al.* Risk factors for hepatocellular carcinoma and its incidence after interferon treatment in patients with chronic hepatitis C. Osaka Liver Disease Study Group. *Hepatology* 1998; **27**: 1394–402.
2 Okanoue T, Itoh Y, Minami M *et al.* Interferon therapy lowers the rate of progression to hepatocellular carcinoma in chronic hepatitis C but not significantly in advanced stage: a retrospective study in 1148 patients. *J Hepatol* 1999; **30**: 653–9.
3 Ikeda K, Saitoh S, Arase Y *et al.* Effect of interferon therapy on hepatocellular carcinogenesis in patients with chronic hepatitis C: a long-term observation study of 1643 patients using statistical bias correction with proportional hazard analysis. *Hepatology* 1999; **29**: 11–19.
4 Yoshida H, Shiratori Y, Moriyama M *et al.* Interferon therapy reduced the risk for hepatocellular carcinoma: national surveillance program of cirrhotic and noncirrhotic patients with chronic hepatitis C in Japan. IHIT Study Group. Inhibition of hepatocarcinogenesis by interferon therapy. *Ann Inter Med* 1999; **131**: 174–81.
5 Tanaka H, Tsukuma H, Kasahara A *et al.* Effect of interferon therapy on the incidence of hepatocellular carcinoma and mortality of patients with chronic hepatitis C: retrospective cohort study of 738 patients. *Int J Cancer* 2000; **87**: 741–9.
6 Okanoue T, Itoh Y, Kirishima T *et al.* Transient biochemical response in interferon therapy decreases the development of hepatocellular carcinoma for five years and improves the long-term survival of chronic hepatitis C patients. *Hepatol Res* 2002; **23**: 62–77.
7 Serfaty L, Nousbaum JB, Elghouzzi MH, Giral P, Legendre C, Poupon R. Prevalence, severity, and risk factors of liver disease in blood donors positive in a second-generation anti-hepatitis C virus screening test. *Hepatology* 1995; **21**: 330–7.
8 Piton A, Poynard T, Imbert-Bismut F *et al.* Factors associated with serum alanine transaminase activity in healthy subjects: consequences for patients with chronic hepatitis C. *Hepatology* 1998; **27**: 1213–19.
9 Alberti A, Noventa F, Benvegnu L, Boccata S, Gatta A. Prevalence of liver disease in a population of asymptomatic individuals with hepatitis C virus infection. *Ann Intern Med* 2002; **137**: 961–4.
10 Tassopoulos NC. Treatment in patients with normal ALT levels. European Association for the Study of the Liver (EASL) International Conference on Hepatitis C, Paris, February 26–27, 1999. *J Hepatol* 1999; **30**: 956–61.
11 Marcellin P, Levy S, Erlinger S. Therapy of hepatitis C: patients with normal aminotransferase levels. *Hepatology* 1997; **26**: 133S–6.
12 Jamal MM, Soni A, Quinn PG, Wheeler DE, Arora S, Johnston DE. Clinical features of hepatitis C-infected patients with persistently normal alanine transaminase levels in the Southwestern United States. *Hepatology* 1999; **30**: 1307–11.
13 Nutt AK, Hassan HA, Lindsey J, Lamps LW, Raufman JP. Liver biopsy in the evaluation of patients with chronic hepatitis C who have repeatedly normal or near-normal serum alanine aminotransferase levels. *Ann Intern Med* 2000; **109**: 62–4.
14 Pradat P, Alberti A, Poynard T *et al.* Predictive value of ALT levels for histologic findings in chronic hepatitis C: a European collaborative study. *Hepatology* 2002; **36**: 973–7.
15 Hui CK, Monto A, Belaye T, Lau E, Wright TL. Outcomes of interferon alpha and ribavirin treatment for chronic hepatitis C in patients with normal serum aminotransferase. *Gut* 2003; **52**: 1644–8.
16 Renou C, Halfon P, Pol S *et al.* Histological features and HLA class II alleles in hepatitis C virus chronically infected

patients with persistently normal alanine aminotransferse levels. *Gut* 2002; **51**: 585–90.
17 Okanoue T, Yasui K, Sakamoto S *et al.* Circulating HCV RNA, HCV genotype, and liver histology in asymptomatic individuals reactive for anti-HCV antibody and their follow-up study. *Liver* 1996; **16**: 241–7.
18 Okanoue T, Makiyama A, Nakayama M *et al.* A follow-up study to determine the value of liver biopsy and need for antiviral therapy for hepatitis C virus carriers with persistently normal serum aminotransferase. *J Hepatol* 2005; **43**: 599–605.
19 Bacon BR. Treatment of patients with hepatitis C and normal serum aminotransferase levels. *Hepatology* 2002; **36**: S179–84.
20 Zeuzem S, Diago M, Gane E *et al.* Peginterferon alfa-2a (40 kilodaltons) and ribavirin in patients with chronic hepatitis C and normal aminotransferase levels. *Gastroenterology* 2004; **127**: 1724–32.
21 Manns MP, McHutchison JG, Gordon SC *et al.* Peginterferon alfa-2b plus ribavirin compared to interferon alfa-2b plus ribavirin for the treatment of chronic hepatitis C: a randomized controlled trial. *Lancet* 2001; **359**: 958–65.
22 Fried MW, Shiffman ML, Reddy KR *et al.* Peginterferon alfa-2a plus ribavirin for chronic hepatitis C virus infection. *N Engl J Med* 2002; **347**: 975–82.
23 Puoti C, Magrini A, Stati T *et al.* Clinical, histological, and virological features of hepatitis C virus carriers with persistently normal or abnormal alanine aminotransferase levels. *Hepatology* 1997; **26**: 1393–8.
24 Prati D, Taidoli E, Zanela A *et al.* Updated definition of healthy ranges for serum alanine aminotransferase levels. *Ann Intern Med* 2002; **137**: 1–9.
25 Desmet VJ, Gerber M, Hoofnagle JH *et al.* Classification of chronic hepatitis: diagnosis, grading and staging. *Hepatology* 1994; **19**: 1513–20.
26 Ishak K, Baptista L, Bianchi L *et al.* Histological grading and staging of chronic hepatitis. *J Hepatol* 1995; **22**: 696–9.
27 MacSween RNM, Anthony PP, Sheuer PJ. *Pathology of the Liver*. Edinburgh: Churchill Livingstone, 1987.
28 Tsukiyama-Kohara K, Yamaguchi K, Maki N *et al.* Antigenicities of group 1 and 2 hepatitis C virus polypeptides: molecular basis of diagnosis. *Virology* 1993; **192**: 430–7.
29 Simmonds P, Alberti A, Alter HJ *et al.* A proposed system for the nomenclature of hepatitis C virus genotypes. *Hepatology* 1994; **19**: 1321–4.
30 Makiyama A, Itoh Y, Kasahara A *et al.* Characteristics of patients with chronic hepatitis C who develop hepatocellular carcinoma after sustained response to interferon. *Cancer* 2004; **101**: 1616–22.
31 Healey CJ, Chapman RWG, Fleming KA. Liver histology in hepatitis C virus infection: a comparison between patients with persistently normal or abnormal transaminase. *Gut* 1993; **37**: 274–8.
32 Ohkoshi S, Tawaraya H, Kuwana K *et al.* A retrospective study of hepatitis C virus carriers in a local endemic town in Japan. *Dig Dis Sci* 1995; **40**: 465–71.
33 Puoti C, Castellacci R, Montagness F *et al.* Histological and virological features and follow-up of HCV carriers with normal aminotransferase levels: the Italian Study of the Asymptomatic C Carriers (ISACC). *J Hepatol* 2002; **37**: 117–23.
34 Yano M, Kumada H, Kage M *et al.* The long-term pathological evolution of chronic hepatitis C. *Hepatology* 1996; **332**: 1463–6.
35 Poynard T, Bedossa P, Opolon P. Natural history of liver fibrosis progression in patients with chronic hepatitis C. The OBSVIRC, METAVIR, CLINVIR, and DOSVIRC. *Lancet* 1997; **346**: 825–32.
36 Takahashi M, Yamada G, Miyamoto R, Doi H, Endo H, Tsuji T. Natural course of chronic hepatitis C. *Am J Gastroenterol* 1993; **88**: 240–3.
37 Ghany MG, Kleiner DE, Alter H *et al.* Progression of fibrosis in chronic hepatitis C. *Gastroenterology* 2003; **124**: 97–104.
38 Mathurin P, Moussalli J, Cardanei J-F *et al.* Slow progression rate of fibrosis in hepatitis C virus patients with persistently normal alanine transaminase activity. *Hepatology* 1998; **27**: 868–72.
39 Hui C-K, Belaye T, Montegrade K, Wright TL. A comparison in the progression of liver fibrosis in chronic hepatitis C between persistently normal and elevated transaminase. *J Hepatol* 2003; **38**: 511–17.
40 Prati D, Shiffman ML, Diago M *et al.* Viral and metabolic factors influencing alanine aminotransferase activity in patients with chronic hepatitis C. *J Hepatol* 2006; **44**: 679–85.
41 Tarao K, Ohkawa S, Tamai S, Miyakawa K. Sustained low serum GPT level below 80 INU in HCV- associated cirrhotic patients by multiagents prevent development of hepatocellular carcinoma. *Cancer* 1994; **73**: 1149–54.
42 Boccato S, Pistis R, Noventa F, Guido M, Benvegnu L, Alberti A. Fibrosis progression in initially mild chronic hepatitis C. *J Viral Hepat* 2006; **13**: 297–302.
43 Cadranel JF, Rufat P, Degos F. Practices of liver biopsy in France: results of a prospective nationwide survey. For the Group of Epidemiology of the French Association for the Study of the Liver (AFEF). *Hepatology* 2000; **32**: 477–81.
44 Castera L, Negre I, Samii K, Buffet C. Pain experienced during percutaneous liver biopsy. *Hepatology* 1999; **30**: 1529–30.
45 Afdal NH. Diagnosing fibrosis in hepatitis C: is the pendulum swinging from biopsy to blood test? *Hepatology* 2003; **37**: 972–4.
46 Imbert-Bismut F, Ratziu V, Pieroni L, Charlotte F, Benhamou Y, Poynard T. Biochemical markers of liver fibrosis in patients with hepatitis C virus infection: a prospective study. *Lancet* 2001; **357**: 1069–75.

47 Sandrin L, Fourquet B, Hasquenoph JM *et al.* Transient elastography: a new invasive method for assessment of hepatic fibrosis. *Ultrasound Med Biol* 2003; **29**: 1705–13.
48 Castera L, Vergniol J, Foucher J *et al.* Prospective comparison of transient elastography, fibrotest, APRI, and liver biopsy for the assessment of fibrosis in chronic hepatitis C. *Gastroenterology* 2005; **128**: 343–50.
49 Saito H, Tada S, Nakamoto N *et al.* Efficacy of non-invasive elastometry on staging of hepatic fibrosis. *Hepatol Res* 2004; **29**: 97–103.
50 Colletta C, Smirne C, Fabris C *et al.* Value of two noninvasive methods to detect progression of fibrosis among HCV carriers with normal aminotransferase. *Hepatology* 2005; **42**: 838–645.
51 Castera L, Foucher J, Bertet J, Couzigou P. FibroScan and FibroTest to assess liver fibrosis in HCV with normal aminotransferse. *Hepatology* 2006; **43**: 373–4.
52 Alberti A. Towards more individualized management of hepatitis V virus patients with initially or persistently normal alanineaminotransferase levels. *J Hepatol* 2005; **42**: 266–74.

GENES, CHROMOSOMES & CANCER 48:109–120 (2009)

RESEARCH ARTICLES

ERK5 is a Target for Gene Amplification at 17p11 and Promotes Cell Growth in Hepatocellular Carcinoma by Regulating Mitotic Entry

Keika Zen,[1] Kohichiroh Yasui,[1]* Tomoaki Nakajima,[1] Yoh Zen,[2] Kan Zen,[3] Yasuyuki Gen,[1] Hironori Mitsuyoshi,[1] Masahito Minami,[1] Shoji Mitsufuji,[1] Shinji Tanaka,[4] Yoshito Itoh,[1] Yasuni Nakanuma,[2] Masafumi Taniwaki,[5] Shigeki Arii,[4] Takeshi Okanoue,[1] and Toshikazu Yoshikawa[1]

[1]Molecular Gastroenterology and Hepatology, Graduate School of Medical Science, Kyoto Prefectural University of Medicine, Kyoto, Japan
[2]Department of Human Pathology, Kanazawa University Graduate School of Medicine, Kanazawa, Japan
[3]Division of Cardiovascular Medicine, Omihachiman Community Medical Center, Omihachiman, Japan
[4]Department of Hepato-Biliary-Pancreatic Surgery, Tokyo Medical and Dental University, Tokyo, Japan
[5]Molecular Hematology and Oncology, Graduate School of Medical Science, Kyoto Prefectural University of Medicine, Kyoto, Japan

Using high-density oligonucleotide microarrays, we investigated DNA copy-number aberrations in cell lines derived from hepatocellular carcinomas (HCCs) and detected a novel amplification at 17p11. To identify the target of amplification at 17p11, we defined the extent of the amplicon and examined HCC cell lines for expression of all seven genes in the 750-kb commonly amplified region. Mitogen-activated protein kinase (MAPK) 7, which encodes extracellular-regulated protein kinase (ERK) 5, was overexpressed in cell lines in which the gene was amplified. An increase in *MAPK7* copy number was detected in 35 of 66 primary HCC tumors. Downregulation of *MAPK7* by small interfering RNA suppressed the growth of SNU449 cells, the HCC cell line with the greatest amplification and overexpression of *MAPK7*. ERK5, phosphorylated during the G2/M phases of the cell cycle, regulated entry into mitosis in SNU449 cells. In conclusion, our results suggest that *MAPK7* is likely the target of 17p11 amplification and that the ERK5 protein product of *MAPK7* promotes the growth of HCC cells by regulating mitotic entry.

INTRODUCTION

Hepatocellular carcinoma (HCC) is the fifth most common malignancy in the world and is estimated to cause approximately half a million deaths annually (El-Serag, 2002). Several risk factors for HCC have been reported, including infection with hepatitis B and C viruses, dietary intake of afratoxin, alcohol consumption, and diabetes.

The mitogen-activated protein kinase (MAPK) cascades transmit extracellular signals from cell surface receptors to specific intracellular targets and regulate a wide variety of cellular functions, including cell proliferation, differentiation, and the stress response (Nishimoto and Nishida, 2006). Extracellular stimuli induce sequential activation of MAPK kinase kinase, MAPK kinase, and MAPK. At least four MAPK subfamilies have been identified: extracellular-regulated protein kinase (ERK) 1 and 2, c-Jun-N-terminal kinases, p38, and ERK5 (also know as BMK1). ERK5, which was recently characterized, can be activated by a wide range of growth factors and cellular stresses, including serum, epithelial growth factor, oxidative stress, and hyperosmotic shock (Hayashi and Lee, 2004; Nishimoto and Nishida, 2006; Wang and Tournier, 2006). When stimulated, MAP/ERK kinase kinase 2 and 3 activate MAP/ERK kinase (MEK) 5, a specific kinase for ERK5. Subsequently, MEK5 phosphorylates ERK5, and the activated ERK5 promotes cell proliferation, differentiation, and survival (Hayashi and Lee, 2004; Garaude et al., 2006; Nishimoto and Nishida, 2006; Wang and Tournier, 2006). Some investigators have described the possible involvement of ERK5 in cancers (Esparis-Ogando et al., 2002; Weldon et al., 2002; Mulloy et al., 2003; Carvajal-Vergara et al., 2005; Linnerth et al., 2005).

Additional Supporting Information may be found in the online version of this article.

Supported by: Grants-in-Aid for Scientific Research from the Japan Society for the Program of Science, Grant number: 18390223.

*Correspondence to: Kohichiroh Yasui, Molecular Gastroenterology and Hepatology, Graduate School of Medical Science, Kyoto Prefectural University of Medicine, 465 Kajii-cho, Kamigyo-ku, Kyoto, 602-8566, Japan. E-mail: yasuik@koto.kpu-m.ac.jp

Received 24 May 2008; Accepted 11 September 2008
DOI 10.1002/gcc.20624
Published online 30 October 2008 in Wiley InterScience (www.interscience.wiley.com).

Accumulating evidence suggests that multiple sequential genetic alterations in a cell lineage at the nucleotide and chromosome levels underlie the carcinogenesis of solid tumors. Amplification of chromosomal DNA is one mechanism of activating genes whose overexpression contributes to the development and progression of cancer. Regions of chromosomal amplification in cancer cells frequently harbor oncogenes, such as *MYC* (Little et al., 1983) and *ERBB2* (Di Fiore et al., 1987). Using comparative genomic hybridization (CGH), we have detected novel regions of amplification in a variety of cancer types, including HCC, and we have identified a number of candidate oncogenes from amplicons (Yasui et al., 2001; Yasui et al., 2002; Yokoi et al., 2002; Okamoto et al., 2003; Yokoi et al., 2003). CGH was initially used for genome-wide detection of copy number changes occurring in cancers (Kallioniemi et al., 1992). However, its resolution is limited (5–10 Mb) because it detects segmental copy number changes on metaphase chromosomes.

The recent introduction of high-density oligonucleotide microarrays designed for typing of single nucleotide polymorphisms (SNPs) facilitates high-resolution mapping of chromosomal amplifications, deletions, and loss of heterozygosity (Mei et al., 2000; Bignell et al., 2004; Matsuzaki et al., 2004a,b; Wong et al., 2004; Zhao et al., 2004). The Affymetrix GeneChip Mapping 100K array set contains 116,204 SNP loci with a mean intermarker distance of 23.6 kb, and it enables detailed and genome-wide identification of DNA copy number changes (Matsuzaki et al., 2004a,b; Garraway et al., 2005; Zhao et al., 2005). The newer GeneChip Mapping 500K array set is composed of two arrays, each capable of genotyping an average 250,000 SNPs.

In the work reported here, we investigated DNA copy number aberrations in HCC cell lines using Affymetrix high-density SNP arrays. We identified a novel amplification at 17p11 in HCC cell lines. This region may harbor one or more genes that, when amplified, contribute to carcinogenesis. Within the amplicon, *MAPK7*, which encodes ERK5, emerged as a probable target gene that acts as a driving force for amplification of the region and promotes the growth of HCC cells by regulating entry into mitosis.

MATERIALS AND METHODS

Cell Lines and Tumor Samples

A total of 21 liver cancer cell lines [HCC-derived HLE, HLF (Dor et al., 1975), PLC/PRF/5 (Alexander et al., 1976), Li7 (Hirohashi et al., 1979), Huh7 (Nakabayashi et al., 1982), Hep3B (Aden et al., 1979), SNU354, SNU368, SNU387, SNU398, SNU423, SNU449, SNU475 (Park et al., 1995), JHH-1, JHH-2, JHH-4, JHH-5, JHH-6, JHH-7 (Fujise et al., 1990), Huh-1 (Huh et al., 1981), and the hepatoblastoma line HepG2 (Knowles et al., 1980)] were examined in this study. All cell lines were maintained in Dulbecco's modified Eagle's medium supplemented with 10% fetal bovine serum. We obtained 66 primary HCC tumors for analysis of the DNA copy number of *MAPK7* from patients undergoing surgery at the hospitals of Tokyo Medical and Dental University and Kyoto University, Japan. Genomic DNA was isolated from each cell line and from 66 primary tumors using the Puregene DNA isolation kit (Gentra, Minneapolis, MN). For immunohistochemical studies of ERK5, 43 additional HCC samples were obtained from the Hospital of Kyoto Prefectural University of Medicine, Japan. Before initiation of the present study, informed consent was obtained in the formal style approved by all relevant ethical committees.

SNP Assay

The GeneChip Mapping 100K array set and GeneChip Mapping 250K Sty array (Affymetrix, Santa Clara, CA) were used in this study. Analyses were performed according to the manufacturer's instructions. In brief, 250 ng of genomic DNA was digested with a restriction enzyme (*Xba*I or *Hind*III for the 100K array set and *Sty*I for the 250K Sty array), ligated to an adaptor, and amplified by PCR (Kennedy et al., 2003; Matsuzaki et al., 2004a,b; Zhao et al., 2004). Amplified products were fragmented, labeled by biotinylation, and hybridized to the microarrays. Hybridization was detected by incubation with a streptavidin-phycoerythrin conjugate, followed by scanning of the array, and analysis was performed as described previously (Kennedy et al., 2003; Di et al., 2005). Copy number changes were calculated using the Copy Number Analyzer for Affymetrix GeneChip Mapping Arrays (http://www.genome.umin.jp) (Nannya et al., 2005).

Fluorescence In Situ Hybridization

We performed FISH using the bacterial artificial chromosome (BAC) RP11-73E4 as a probe (Invitrogen, Carlsbad, CA) as described previously (Yasui et al., 2002). The BAC was selected

on the basis of its location according to the database provided by the UCSC (http://genome.ucsc.edu/). Briefly, the probe was labeled by nick translation with biotin-16-dUTP (Roche Diagnostics, Penzberg, Germany) and hybridized to metaphase chromosomes. Hybridization signals for biotin-labeled probes were detected with avidin-fluorescein (Roche Diagnostics).

Real-Time Quantitative PCR

We quantified genomic DNA and mRNA using a real-time fluorescence detection method. Total RNA was obtained using Trizol (Invitrogen). Residual genomic DNA was removed by incubating the RNA samples with RNase-free DNase I (Takara Bio, Shiga, Japan) prior to reverse transcription (RT)-PCR. Single-stranded complementary DNA was generated using superscript III reverse transcriptase (Invitrogen) according to the manufacturer's directions. Real-time quantitative PCR experiments were performed with the LightCycler system using FastStart DNA Master Plus SYBR Green I (Roche Diagnostics) according to the manufacturer's protocol. The primers were as follows: *MAPK7* DNA (forward, 5′-TGCTGACTGGCTCGAAG-3′; reverse, 5′-GGGTCTGAGATGAACCTGC-3′); *MAPK7* mRNA (forward, 5′-TTTGCCTTACTTCCCACCTG-3′; reverse, 5′-CCCATGTCGAAAGACTGGTT-3′); *GRAP* mRNA (forward, 5′-TCGAAGGACAGACTGCACAC-3′; reverse, 5′-AGAAGAGGAGTGTGCCTCCA-3′); *EPN2* mRNA (forward, 5′-TCACCTCACCCACCACTGTA-3′; reverse, 5′-GTGGTCAGCTGCCCTTAGAG-3′); *EPPB9* mRNA (forward, 5′-CTTTGTGTACGGCCAGGACT-3′; reverse, 5′-CGTAGGGGTTGGTGCTTTTA-3′); *MFAP4* mRNA (forward, 5′-GGTGACTCCCTGTCCTACCA-3′; reverse, 5′-TCATCTCAGTGCGTTTGAGG-3′); *ZNF179* mRNA (forward, 5′-ACTGGGCAGAACCAGAGAGA-3′; reverse, 5′-AGGATGCACAGACAGGCTCT-3′); *FLJ10847* mRNA (forward, 5′-AACTCTTGGGCTTCAAGCAA-3′; reverse, 5′-AGGAGGTTGAGGCTGCAGTA -3′). These primers were designed using Primer3 (http://frodo.wi.mit.edu/cgi-bin/primer3/primer3_www.cgi) on the basis of sequence data obtained from the NCBI database (http://www.ncbi.nlm.nih.gov/). *GAPDH* (Minamiya et al., 2004) and long interspersed nuclear element (LINE)-1 (Zhao et al., 2004) were used as endogenous controls for mRNA and genomic DNA levels, respectively.

Immunoblotting

Immunoblots were prepared according to previously reported methods (Yasui et al., 2001). Cell lysates (20 μg protein per sample) were separated by sodium dodecyl sulfate-polyacrylamide gel electrophoresis on 10% acrylamide gels. We obtained the following antibodies from Sigma-Aldrich (Tokyo, Japan): anti-ERK5 polyclonal antibody, anti-phospho-ERK5 (pThr218/pThr220) polyclonal antibody, and anti-β-actin monoclonal antibody. For immunoblotting, we used anti-ERK5, anti-phospho-ERK5, and anti-β-actin at dilutions of 1:500, 1:1000, and 1:5000, respectively. For secondary immunodetection, we used anti-rabbit or anti-mouse Ig (Amersham, Tokyo, Japan) diluted 1:5000. Protein binding was detected using the ECL system (Amersham).

Immunoprecipitation

Cells were lysed with RIPA buffer (10 mM Tris-HCl, pH 7.4, 150 mM NaCl, 1% Triton X-100, 0.1% sodium dodecyl sulfate, 1% sodium deoxycholate, 1 mM phenylmethylsulfonyl fluoride), and incubated on ice for 30 min. The lysate was centrifuged at 14,000 × *g* at 4°C for 15 min. The supernatant was incubated with normal rabbit IgG and protein A-agarose beads (Santa Cruz Biotechnology, Santa Cruz, CA) to decrease nonspecific protein binding. After centrifugation, the supernatant was incubated with anti-ERK5 polyclonal antibody or normal rabbit IgG (control) overnight at 4°C. Protein A-agarose beads were added to the reaction and the mixture was incubated for an additional 1 hr. The precipitates were recovered by a brief centrifugation, followed by four washes with RIPA buffer. Samples were then boiled in electrophoresis sample buffer and separated by electrophoresis as described above (see "Immunoblotting" section).

Immunohistochemical Analysis

Forty-three primary HCCs, consisting of paired tumor and surrounding nontumor tissues, and two HCC cell lines (SNU449 and Li7) were analyzed by anti-ERK5 immunostaining. Immunohistochemical staining was performed on formalin-fixed and paraffin-embedded sections using an anti-ERK5 polyclonal antibody (Sigma-Aldrich) at a 1:200 dilution. An automated tissue immunostainer (Ventana Medical Systems, Tucson, AZ) was used according to the manufacturer's instructions. The staining was developed with 3,3′-

diaminobenzidine tetrahydrochloride, followed by counterstaining with hematoxylin.

Growth Assays and RNA Interference Studies

For cell growth assays viable cells were stained with 0.2% trypan blue and counted with a hemocytometer 24, 48, and 72 hr after transfection. For RNA interference (RNAi) studies, Stealth small interfering RNA (siRNA) duplex oligoribonucleotides targeting *MAPK7* (5′-CCAUGGCAUGAAC CCUGCCGAUAUU-3′) and Stealth RNAi negative control duplexes were synthesized by Invitrogen. The siRNAs were delivered into SNU449 cells using Lipofectamine 2000 (Invitrogen) according to the manufacturer's instructions. To determine mRNA levels, cells were harvested 48 hr after transfection and subjected to quantitative RT-PCR as described above.

Cell Cycle Synchronization

SNU449 cells were synchronized at G1/S, early S, or M phases. For G1/S or early S-phase synchronization, cells were incubated in medium containing 2.5 mM thymidine (Sigma Chemical Co., St. Louis, MO) for 24 hr, followed by 12 hr in medium without thymidine, and finally another 12 hr in medium containing 2.5 mM thymidine (double-thymidine block; for G1/S-phase) or 1 μg/ml aphidicolin (early S-phase block). For M phase synchronization, cells were incubated in medium containing 2.5 mM thymidine for 24 hr, followed by 4 hr in medium without thymidine, and finally another 12 hr in medium containing 0.5 μg/ml nocodazole.

Cell Cycle Analysis

SNU449 cells were synchronized at the G1/S-phase boundary by a double-thymidine block as described above. Synchronized cells were released into fresh medium without thymidine and harvested at the indicated time points. These cells were then stained with propidium iodide and analyzed using a FACSCaliber scanner and Cell Quest software (Becton Dickinson Pharmingen, San Diego, CA).

Mitotic Index

Cells were grown in 24-well plates and transfected with Stealth RNAi targeting *MAPK7* or Stealth RNAi negative control duplexes as described above (see "Growth Assays and RNA Interference Studies" section). After 24 hr, cells were synchronized at the G1/S-phase boundary by a double-thymidine block. Synchronized cells were collected, reseeded on glass slides, and incubated for an additional 9 hr in fresh medium without thymidine. Next, the cells were stained with an anti-phospho-histone H3 antibody that specifically detects mitotic cells. Briefly, cells were fixed with 3.7% formaldehyde, permeabilized with 0.25% Triton X-100, and incubated with PBS containing 1% bovine serum albumin. The cells were then treated with a mixture of 4 μg/ml anti-phospho-histone H3 (Ser10)-biotin conjugated antibody (Upstate Biotechnology, Lake Placid, NY) and a 1:100 dilution of streptavidin-fluorescein (Roche Diagnostics) for 1 hr at room temperature, followed by counterstaining with propidium iodide. Positive staining for phospho-histone H3 was quantified by counting stained cells under a fluorescence microscope and dividing by the number of total cells. The mitotic index was scored as the percentage of mitotic cells in a population. On average, 200 cells were scored in three separate areas.

Statistical Analysis

All statistical analyses were performed using SPSS 15.0 software (SPSS Inc., Chicago, IL). Chi-square tests or analysis of variance (ANOVA) were used. P values < 0.05 were considered significant.

RESULTS

Detection of the 17p11 Amplicon in HCC Cell Lines by SNP Array Analysis

We screened for DNA copy number aberrations in 20 HCC cell lines by SNP array analysis. Two of the 20 cell lines, SNU449 and JHH-7, exhibited amplifications at chromosomal band 17p11 (Fig. 1A). In particular, the SNU449 cell line showed a high level of amplification in a narrow region on 17p11. We were able to define the smallest commonly affected region in the 17p11 amplicon as that lying between the positions recognized by the Affymetrix SNP_A-1662618 and SNP_A-1720748 probes (Fig. 1B). This region includes seven known or predicted protein-coding genes, *GRAP*, *EPN2*, *EPPB9*, *MAPK7*, *MFAP4*, *ZNF179*, and *FLJ10847*. The size of the amplicon was estimated to be approximately 750 kb.

To confirm amplification at 17p11 in SNU449 cells, we performed FISH analysis. The probe for

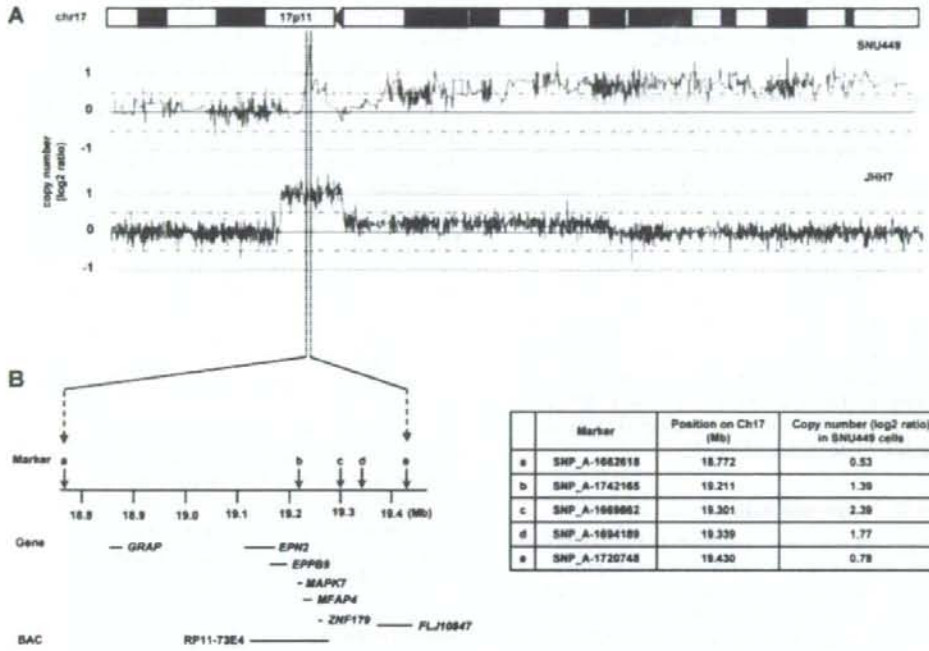

	Marker	Position on Chr17 (Mb)	Copy number (log2 ratio) in SNU449 cells
a	SNP_A-1662618	18.772	0.53
b	SNP_A-1742165	19.211	1.39
c	SNP_A-1669862	19.301	2.39
d	SNP_A-1694189	19.339	1.77
e	SNP_A-1720748	19.430	0.78

Figure 1. Map of the amplicon at 17p11 in two HCC cell lines. A: Copy number profiles for chromosome 17 in SNU449 and JHH-7 cells. Copy number values were determined by SNP 100K and 250K array analyses for SNU449 and JHH-7 cells, respectively. B: The smallest common region of amplification in SNU449 and JHH-7 cells (left). The position of the Affymetrix SNP markers, the seven genes within the amplicon (*GRAP*, *EPN2*, *EPPB9*, *MAPK7*, *MFAP4*, *ZNF179*, and *FLJ10847*) and the BAC RP11-73E4 (used as a probe for FISH) are numbered according to the UCSC genome database (http://genome.ucsc.edu/). Detailed copy-number information at positions identified by individual SNP markers over the amplified region in SNU449 cells is shown at right.

these experiments was BAC RP11-73E4, which contains *EPN2*, *EPPB9*, *MAPK7*, *MFAP4*, and *ZNF179* (Fig. 1B). This probe showed an amplified FISH signal on metaphase chromosomes from SNU449 cells (Fig. 2A). To further characterize the relationship between the genes in this chromosomal region and amplifications observed in cancer cells, we analyzed the gene dosage of the *MAPK7* locus by real-time quantitative PCR of DNA from 21 different liver cancer cell lines (20 HCC cell lines and the hepatoblastoma line HepG2). Amplification of *MAPK7* was observed in SNU449 and JHH-7 cells (Fig. 2B). Taken together, the data provide strong evidence that the 17p11 region is amplified in SNU449 and JHH-7 cells.

Analysis of Positional Candidate Genes in HCC Cell Lines

The 17p11 region may harbor one or more genes (henceforth referred to as "target genes") that, when activated by amplification, play a role in carcinogenesis. A common criterion for designating a gene as a putative target is that amplification leads to its overexpression (Collins et al., 1998). Thus, using real-time quantitative PCR, we determined the mRNA levels of all seven genes in the 17p11 amplicon in our panel of 21 liver cancer cell lines. As shown in Fig. 2C, the *EPN2*, *EPPB9*, and *MAPK7* genes were overexpressed in both SNU449 and JHH-7 cells. In several other lines, one or more of these three genes was overexpressed, despite the fact that regional amplification was not observed. These findings suggest that *EPN2*, *EPPB9*, and *MAPK7* are candidate target genes for 17p11 amplification.

Of these three genes, we chose to focus further analysis on *MAPK7*, which encodes ERK5, because ERK5-related proteins have been previously implicated in carcinogenesis (Hayashi and Lee, 2004; Wang and Tournier, 2006), whereas there is little or no evidence linking *EPN2* or

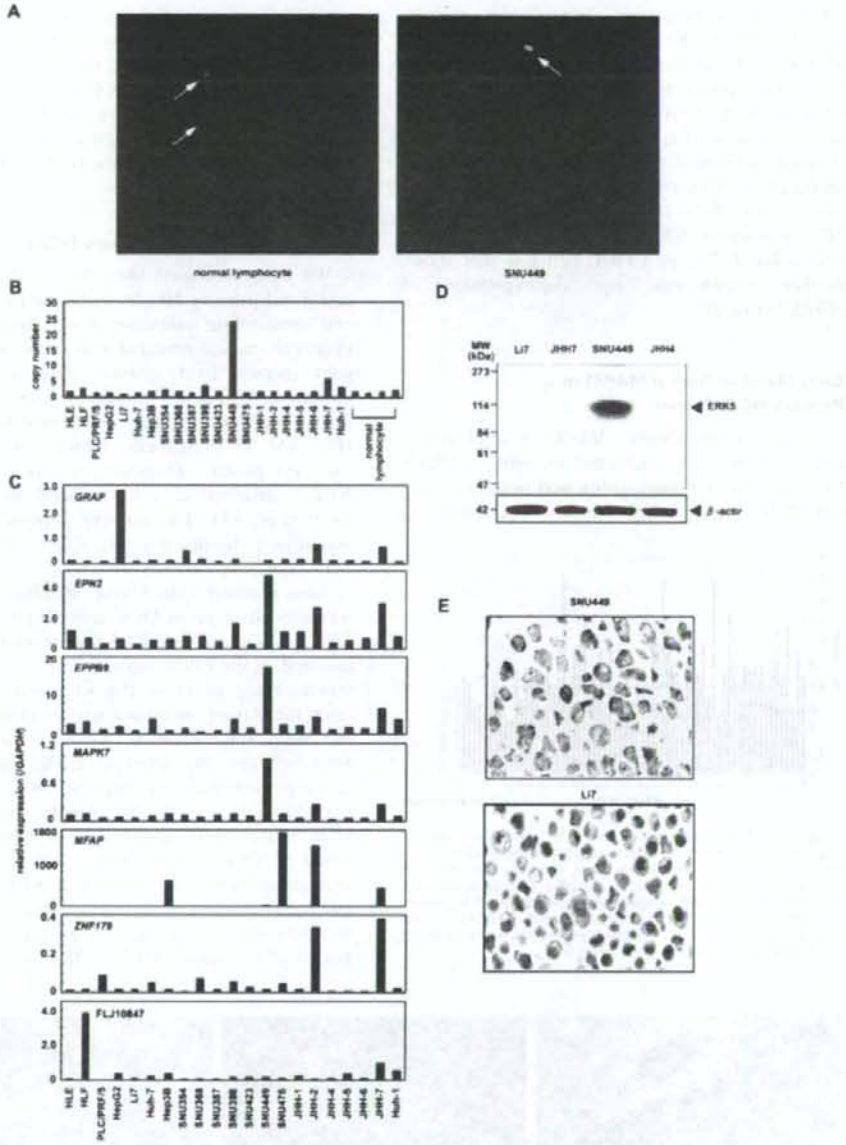

Figure 2. Amplification and overexpression of *MAPK7* in HCC cell lines. (A) Representative images from FISH analysis using a BAC RP11-73E4 probe on metaphase chromosomes from normal lymphocytes and SNU449 cells. While the probe shows a normal signal pattern (2 copies/cell) in normal lymphocytes (arrows, left), it shows an amplified signal in SNU449 cells (arrow, right). (B) Copy number of *MAPK7* in 21 liver cancer cell lines (20 HCC cells and one hepatoblastoma line, HepG2) and four peripheral blood lymphocytes (normal cell controls) as measured by real-time quantitative PCR with reference to a LINE-1 control. Values were normalized such that the average copy number of *MAPK7* in genomic DNA derived from normal lymphocytes is 2. (C) Relative expression levels of the seven genes within the 17p11 amplicon in a panel of 21 liver cancer cell lines as determined by real-time quantitative RT-PCR. The results are presented as the ratio between the expression level of each gene and a reference gene (*GAPDH*) to correct for variation in the amount of RNA. (D) Immunoblot analysis to detect protein levels of ERK5 and β-actin, an internal control, in four HCC cell lines with different *MAPK7* DNA copy numbers (B) and mRNA levels (C). (E) Immunostaining of ERK5 in SNU449 and LI7 cells.

EPPB9 to tumorigenesis. Immunoblot analysis revealed that ERK5 expression is upregulated in SNU449 cells. Indeed, among the HCC cell lines that were tested, SNU449 showed the highest level of both 17p11 amplification and *MAPK7* overexpression (Fig. 2D). Moreover, immunostaining confirmed that the level of ERK5 was elevated in SNU449 cells. ERK5 was strongly expressed in the cytoplasm of SNU449 cells (Fig. 2E). In contrast, ERK5 was weakly expressed in only a few Li7 cells, a HCC cell line that shows neither amplification nor overexpression of *MAPK7* (Fig. 2E).

Copy Number Gain of *MAPK7* in Primary HCC Tumors

To determine whether *MAPK7* is amplified in primary tumors, we examined 66 primary HCCs for copy number gains using real-time quantitative PCR. Copy number changes were counted as gains if the results of the analysis for a given tumor cell type exceeded the mean plus twice the standard deviation (SD) of the levels of *MAPK7* observed in genomic DNA derived from four peripheral blood lymphocyte samples (i.e., normal cells). A copy number gain for *MAPK7* was observed in 35 of the 66 tumors (53%; Fig. 3).

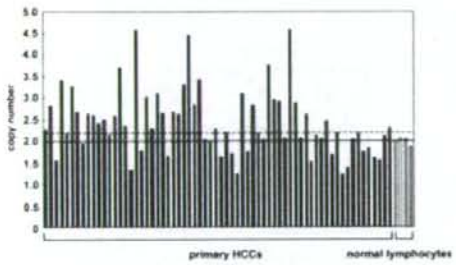

Figure 3. Copy number gain of *MAPK7* in primary HCC tumors. Copy numbers of *MAPK7* in 66 primary HCC tumors and four normal peripheral blood lymphocytes were determined by real-time quantitative PCR with reference to a LINE-1 control. Values were normalized such that the average copy number of *MAPK7* in genomic DNA derived from the normal lymphocytes equals 2 (solid horizontal line). The mean + 2 × SD of normal lymphocytes was used as the cutoff value for copy number gain (dotted line).

Expression of ERK5 in Primary HCCs

We next examined the level of ERK5 in 43 additional primary HCCs, including paired tumor and surrounding nontumor tissues. Immunohistochemical studies revealed that, in nontumor tissues (normal liver, chronic hepatitis, or liver cirrhosis), ERK5 is strongly expressed in bile ducts, bile ductules, and a few small hepatocytes (Fig. 4A). In these cells, ERK5 was present in the cytoplasm. Hepatocytes also contained ERK5, although at a lower level than in bile ducts (Fig. 4A). The staining pattern for ERK5 was almost identical for normal liver, chronic hepatitis, and liver cirrhosis.

This granular cytoplasmic staining for ERK5 was also observed in HCC cancer cells (Fig. 4B). HCC cells containing ERK5 were uniformly distributed in the tumor tissues. The level of ERK5 was elevated in 11 of the 43 tumors compared with the paired nontumor tissues (Figs. 4B and 4C; Supp. Info. Table 1). To clarify the relationship between the level of ERK5 and various clinicopathological parameters, we examined available data from the 43 patients, whose tumors were divided into elevated (T>NT) and not elevated (T≤NT) groups. There was no significant correlation between the level of ERK5 and any parameter examined, including age and gender of the patients; size, stage, and degree of differentiation of the tumor; HBV or HCV infection; and

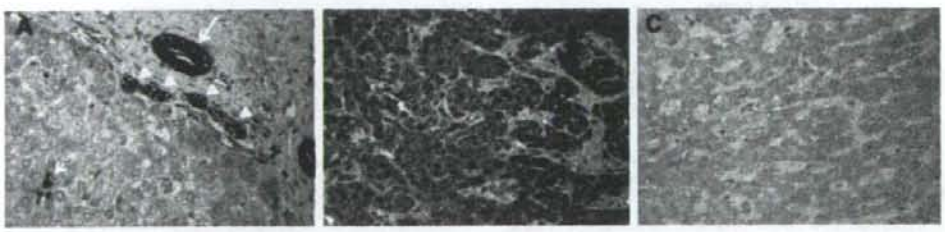

Figure 4. Representative ERK5 immunostaining of tissues. (A) A nontumorous liver tissue (chronic hepatitis). The level of ERK5 is elevated in the bile duct (large arrow), bile ductules (arrowheads), and a few small hepatocytes (small arrow). (B, C) Paired tumor (B) and nontumor (C) tissues from one HCC patient, wherein the level of ERK5 is elevated in the tumor compared with the counterpart nontumor tissue. Original magnification, ×400.

features of nontumorous liver tissues (Supp. Info. Table 1).

Downregulation of *MAPK7* Inhibits the Growth of HCC Cells

To investigate the effects of *MAPK7* overexpression on HCC cells, we knocked down its expression using RNAi. In SNU449 cells treated with siRNA targeting *MAPK7*, we observed a decrease in *MAPK7* mRNA and ERK5 protein levels relative to that observed for cells receiving a control siRNA or transfection agent alone (Figs. 5A and 5B). The siRNA-mediated downregulation of *MAPK7* suppressed the growth of SNU449 cells at all time points assayed over a 72-hr period (Fig. 5C). These findings suggest that ERK5 promotes the growth of HCC cells.

ERK5 is Phosphorylated During the G2/M Phases of the Cell Cycle

To help elucidate the underlying mechanism by which ERK5 regulates cellular proliferation we investigated the role of ERK5 in cell cycle progression. SNU449 cells were synchronized at G1/S, early S, or M phases of the cell cycle using a double-thymidine, aphidicolin, or nocodazole block, respectively. We determined the levels of total ERK5 and phosphorylated (active) form of ERK5. Immunoblotting did not show a difference in the level of total ERK5 among the three phases of the cell cycle (Fig. 6A). To detect phosphorylated ERK5, total ERK5 was immunoprecipitated from cell lysates using an anti-ERK5 antibody and then analyzed by immunoblotting using an anti-phospho-ERK5 antibody. Phosphorylated ERK5 was more abundant in cells synchronized at the M phase than in asynchronous cells (Fig. 6B).

We next synchronized SNU449 cells at the G1/S boundary using a double-thymidine block and then released the cells from the block. Using flow cytometry, we confirmed the synchrony of the cell cycle and monitored its progression after removal of thymidine (Fig. 6C). There was no difference in the level of total ERK5 during progression of the cell cycle (Fig. 6D). Expression of phosphorylated ERK was maximal 9 hr after release from the block (Fig. 6E), a time when a large proportion of cells were in the G2/M phase (Fig. 6C). Taken together, these observations indicate that ERK5 is phosphorylated during the G2/M phases of the cell cycle.

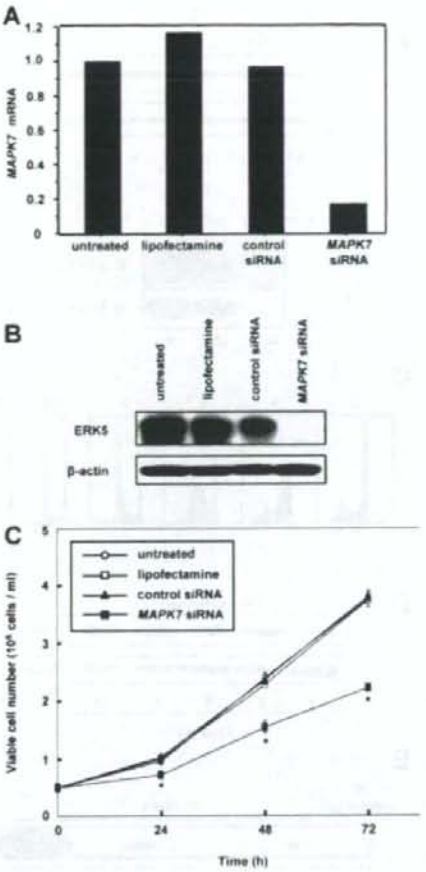

Figure 5. Growth inhibition of SNU449 cells by knockdown of *MAPK7*. A: Relative expression levels of *MAPK7* mRNA as determined by real-time quantitative RT-PCR. SNU449 cells were treated with siRNA targeting *MAPK7*, negative control siRNA, or the transfection agent alone (Lipofectamine), and harvested 48 hr after transfection. Untreated cells were maintained under identical experimental conditions. Results are presented as a ratio between the expression level of *MAPK7* and that of a reference gene (*GAPDH*) to correct for variation in the amount of RNA. Relative expression levels were normalized such that the ratio in untreated cells is 1. B: Levels of ERK5 and β-actin, an internal control, determined by immunoblotting. C: Cell growth was assayed by counting the viable cells at the indicated times after transfection. Each assay was performed in triplicate. Values are represented as the mean ± SD. Differences were analyzed by ANOVA ($^{*}P < 0.01$).

ERK5 Regulates Entry into Mitosis

Our results indicating that ERK5 is activated during the G2/M phases in SNU449 cells suggested that ERK5 may be involved in G2/M progression. To examine whether ERK5 plays a role in mitotic entry, we knocked down *MAPK7*

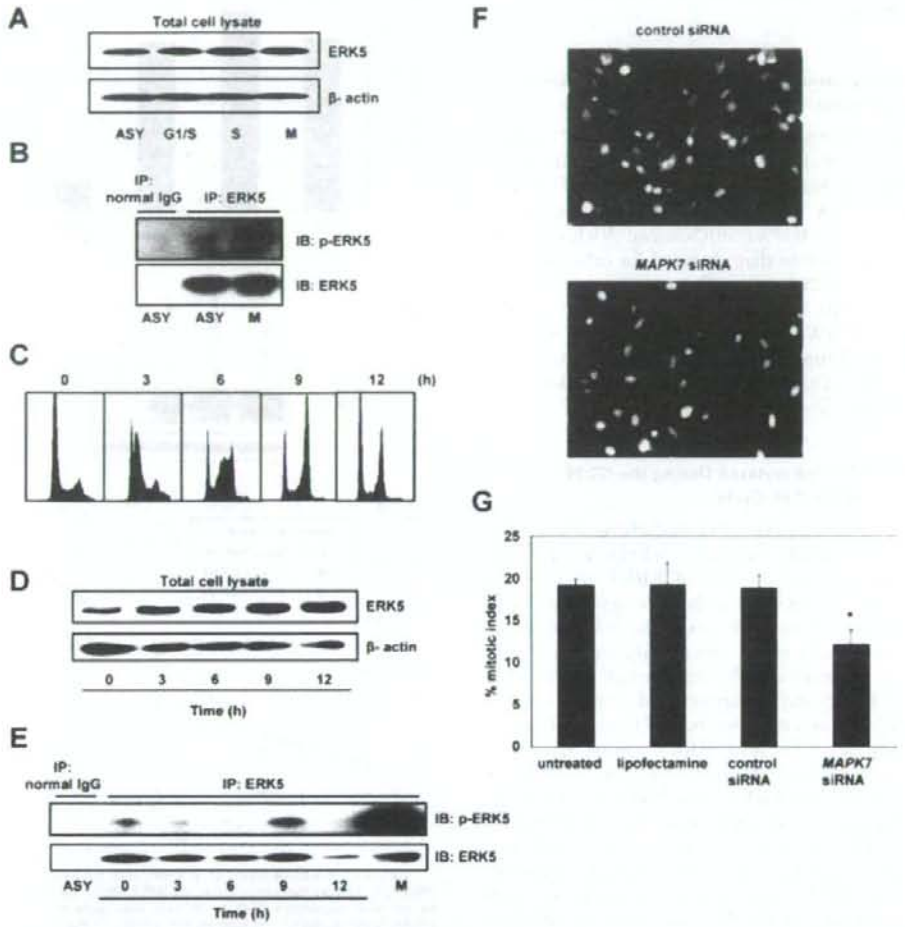

Figure 6. ERK5 is phosphorylated during the G2/M phases of the cell cycle. (A) Immunoblot analysis to detect protein levels of total ERK5 and β-actin, an internal control, in SNU449 cells that were synchronized at the G1/S, early S, or M phases using a double-thymidine, aphidicolin, or nocodazole block, respectively, or were untreated and used as an asynchronous (ASY) population. (B) Levels of phosphorylated ERK5 (p-ERK5). ERK5 was immunoprecipitated (IP) from lysates of SNU449 cells that were synchronized at the M phase (M) or from asynchronous cells (ASY). The samples were split and analyzed by immunoblotting (IB) for p-ERK5 and total ERK5. Normal rabbit immunoglobulin (normal IgG) was used as a negative control for immunoprecipitation. (C) Flow cytometric analysis. SNU449 cells were synchronized to the G1/S boundary using a double-thymidine block. Synchronized cells were released from the block and harvested at the indicated time points. The X-axis indicates DNA content and the Y-axis indicates the number of cells. (D) Time course of changes in the level of total ERK5 after release from the double-thymidine block. The level of β-actin was used as an internal control. (E) Time course of changes in the level of p-ERK5 after release from the double-thymidine block. ERK5 was immunoprecipitated from lysates of SNU449 cells harvested at the indicated times after release from the double-thymidine block. The samples were split and analyzed by immunoblotting for p-ERK5 and total ERK5. SNU449 cells, synchronized at the M phase with nocodazole, were also examined as described in (A) and (B). Normal rabbit IgG was used as a negative control for immunoprecipitation. (F) Representative images of mitotic cells in an SNU449 cell population that was transfected with *MAPK7*- or control-siRNA. SNU449 cells were treated with siRNA targeting *MAPK7*, negative control siRNA, or the transfection agent alone (Lipofectamine). Untreated cell were maintained under identical conditions. These cells were synchronized at the G1/S boundary using a double-thymidine block. The synchronized cells were released from the block and stained with anti-phospho-histone H3 9 hr after release, a time corresponding to the G2/M phase as shown in (C). Mitotic cells were identified by positive staining for phospho-histone H3 (green). Nuclear DNA was stained with propidium iodide (red). (G) The mitotic index was scored as described in Materials and Methods section. Data are presented as means ± SD (ANOVA; $^{*}P < 0.05$).

expression using RNAi and assessed its effect on mitosis. SNU449 cells were transfected with siRNA targeting *MAPK7* and synchronized at the G1/S-phase boundary by a double-thymidine block. The synchronized cells were released from the block and harvested 9 hr after release, a time which corresponds to the G2/M phase (Fig. 6C). Finally, harvested cells were stained with anti-phospho-histone H3 antibody, which specifically detects mitotic cells (Fig. 6F). Compared with a control siRNA or transfection agent alone, transfection of *MAPK7* siRNA significantly reduced the mitotic index (Fig. 6G). These findings suggest that ERK5 regulates mitotic entry in the HCC cells.

DISCUSSION

High-density SNP arrays are powerful tools for high-resolution analysis of DNA copy number aberrations in cancers. In the present study, using the Affymetrix GeneChip 100K and 250K SNP arrays we detected a novel amplification in HCC cells at 17p11. We were able to narrow the amplification to a 750-kb region. Notably, the amplification might have been missed using conventional analyses such as CGH. Amplification at 17p11.2-p12 has been detected in high-grade osteosarcoma using CGH (Forus et al., 1995; Tarkkanen et al., 1995). The group of van Dartel et al., (2002) established 17p11.2-p12 amplification profiles by semi-quantitative PCR using 15 microsatellite markers and seven candidate genes to assay amplification in this tumor type. They found that most of the tumors had complex amplification profiles, suggesting that multiple amplification targets, including *MAPK7*, might be present in region 17p11.2-p12. In contrast, we were able to define a smaller common region of amplification at 17p11 in two HCC cells and to determine the expression status of all genes in the amplicon. Three of the seven genes in the amplicon; *EPN2*, *EPPB9*, and *MAPK7*, were always overexpressed in cells that showed amplification in the 17p11 region. Thus, we considered these three genes as candidate targets for amplification. The function of *EPPB9* (B9 protein) is not known, and the protein encoded by *EPN2* (epsin 2) is similar to epsin 1, which plays a putative role in clathrin-mediated endocytosis (Rosenthal et al., 1999). Therefore, we focused on *MAPK7* as a target for the amplification.

Several lines of evidence implicate ERK5, which is encoded by *MAPK7*, in tumorigenesis (Wang and Tournier, 2006): (a) the ERK5 pathway is activated by Ras (English et al., 1999), ErbB (Esparis-Ogando et al., 2002; Yuste et al., 2005), Src (Sun et al., 2003), Cot (Chiariello et al., 2000), Bcr-Abl (Buschbeck et al., 2005), insulin-like growth factor-II (Linnerth et al., 2005), and interleukin-6 (Carvajal-Vergara et al., 2005); (b) ERK5 is involved in the control of breast cancer cell proliferation (Esparis-Ogando et al., 2002); (c) ERK5 mediates a survival signal that confers chemoresistance to breast cancer (Weldon et al., 2002); (d) insulin-like growth factor-II promotes cell survival via the ERK5 pathway in lung cancer cells (Linnerth et al., 2005); (e) the level of ERK5 contributes to the survival of Bcr/Abl-positive leukemic cells (Buschbeck et al., 2005); (f) ERK5 regulates cell proliferation and antiapoptotic responses in multiple myeloma (Carvajal-Vergara et al., 2005); and (g) an elevated level of MEK5, a specific activator of ERK5, is associated with metastasis and a poor prognosis in prostate cancer (Mehta et al., 2003).

The present study is the first to show the status of amplification and expression of *MAPK7* and its functional role in HCC. We found that *MAPK7* is amplified in 35 of 66 HCC tumors (53%). However, we could not determine the copy number of *MAPK7* in the nontumorous counterparts of the samples assayed because these samples were not available. Therefore, we cannot exclude the possibility that copy number polymorphism might influence the results of copy number analysis. We studied the expression of ERK5 using immunohistochemical analysis in primary HCCs and their surrounding nontumorous liver tissues. In nontumorous liver tissues, ERK5 was weakly expressed in the cytoplasm of non-neoplastic hepatocytes. Intriguingly, it was more strongly expressed in bile ducts, bile ductules, and a few small hepatocytes. In HCC tumor tissues, ERK5 was expressed in the cytoplasm of tumor cells. The level of ERK5 was elevated in 11 of 43 HCC tumors compared with their nontumorous counterparts. However, we did not observe a significant link between the level of ERK5 and any clinicopathological parameters. A recent report showed that, in prostate cancer, an increase in ERK5 cytoplasmic signals correlates with advanced disease and that strong nuclear ERK5 localization correlates with poor survival (McCracken et al., 2008).

We examined the functional roles of ERK5 in HCC cells using RNAi. Downregulation of *MAPK7* by siRNA suppressed the growth of

SNU449 cells, which had the greatest amplification and overexpression of *MAPK7* of all of the cell lines tested. These findings suggest that increased levels of ERK5 enhance the growth of HCC cells. Moreover, our results indicate that ERK5 is phosphorylated during the G2/M phases of the cell cycle and that it regulates entry into mitosis, which may explain how it promotes the growth of HCC cells.

Conflicting results have been reported by different investigators regarding the role of ERK5 in cell cycle progression. Some investigators have reported that ERK5 regulates the G1/S transition: expression of a dominant-negative form of ERK5 prevents cells from entering the S-phase of the cell cycle (Kato et al., 1998), and ERK5 can drive cyclin D1 expression (Mulloy et al., 2003). In contrast, Cude et al., (2007) and Gírio et al., (2007) recently reported that ERK5 is activated at the G2/M phases and is required for mitotic entry, findings that agree with our results.

Few molecules have been identified as direct downstream targets of ERK5. The transcriptional factors of the monocyte enhancer factor 2 family are among the best characterized substrates of ERK5. Phosphorylation of monocyte enhancer factor 2C by ERK5 enhances its transcriptional activity and subsequently leads to an increase in c-Jun gene expression (Kato et al., 1997; Wang and Tournier, 2006). A more complete identification of components downstream of ERK5 will be necessary to fully understand the role of ERK5 in carcinogenesis.

In summary, using high-density SNP arrays, we identified *MAPK7* as a probable target for the amplification events at 17p11 in HCCs. Our results suggest that the ERK5 protein product of the *MAPK7* gene plays a role in proliferation of HCC cells by regulating mitotic entry and may therefore be an optimal target for the development of novel therapies for this widespread type of cancer.

REFERENCES

Aden DP, Fogel A, Plotkin S, Damjanov I, Knowles BB. 1979. Controlled synthesis of HBsAg in a differentiated human liver carcinoma-derived cell line. Nature 282:615–616.

Alexander JJ, Bey EM, Geddes EW, Lecatsas G. 1976. Establishment of a continuously growing cell line from primary carcinoma of the liver. S Afr Med J 50:2124–2128.

Bignell GR, Huang J, Greshock J, Watt S, Butler A, West S, Grigorova M, Jones KW, Wei W, Stratton MR, Futreal PA, Weber B, Shapero MH, Wooster R. 2004. High-resolution analysis of DNA copy number using oligonucleotide microarrays. Genome Res 14:287–295.

Buschbeck M, Hofbauer S, Di Croce L, Keri G, Ullrich A. 2005. Abl-kinase-sensitive levels of ERK5 and its intrinsic basal activity contribute to leukaemia cell survival. EMBO Rep 6:63–69.

Carvajal-Vergara X, Tabera S, Montero JC, Esparís-Ogando A, López-Pérez R, Mateo G, Gutiérrez N, Parmo-Cabañas M, Teixidó J, San Miguel JF, Pandiella A. 2005. Multifunctional role of Erk5 in multiple myeloma. Blood 105:4492–4499.

Chiariello M, Marinissen MJ, Gutkind JS. 2000. Multiple mitogen-activated protein kinase signaling pathways connect the cot oncoprotein to the c-jun promoter and to cellular transformation. Mol Cell Biol 20:1747–1758.

Collins C, Rommens JM, Kowbel D, Godfrey T, Tanner M, Hwang SI, Polikoff D, Nonet G, Cochran J, Myambo K, Jay KE, Froula J, Cloutier T, Kuo WL, Yaswen P, Dairkee S, Giovanola J, Hutchinson GB, Isola J, Kallioniemi OP, Palazzolo M, Martin C, Ericsson C, Pinkel D, Albertson D, Li WB, Gray JW. 1998. Positional cloning of ZNF217 and NABC1: Genes amplified at 20q13.2 and overexpressed in breast carcinoma. Proc Natl Acad Sci USA 95:8703–8708.

Cude K, Wang Y, Choi HJ, Hsuan SL, Zhang H, Wang CY, Xia Z. 2007. Regulation of the G2-M cell cycle progression by the ERK5-NFkappaB signaling pathway. J Cell Biol 177:253–264.

Di Fiore PP, Pierce JH, Kraus MH, Segatto O, King CR, Aaronson SA. 1987. erbB-2 is a potent oncogene when overexpressed in NIH/3T3 cells. Science 237:178–182.

Di X, Matsuzaki H, Webster TA, Hubbell E, Liu G, Dong S, Bartell D, Huang J, Chiles R, Yang G, Shen MM, Kulp D, Kennedy GC, Mei R, Jones KW, Cawley S. 2005. Dynamic model based algorithms for screening and genotyping over 100 K SNPs on oligonucleotide microarrays. Bioinformatics 21:1958–1963.

Dor I, Namba M, Sato J. 1975. Establishment and some biological characteristics of human hepatoma cell lines. Gann 66:385–392.

El-Serag HB. 2002. Hepatocellular carcinoma: An epidemiologic view. J Clin Gastroenterol 35:S72–S78.

English JM, Pearson G, Hockenberry T, Shivakumar L, White MA, Cobb MH. 1999. Contribution of the ERK5/MEK5 pathway to Ras/Raf signaling and growth control. J Biol Chem 274:31588–1592.

Esparís-Ogando A, Díaz-Rodríguez E, Montero JC, Yuste L, Crespo P, Pandiella A. 2002. Erk5 participates in neuregulin signal transduction and is constitutively active in breast cancer cells overexpressing ErbB2. Mol Cell Biol 22:270–285.

Forus A, Weghuis DO, Smeets D, Fodstad O, Myklebost O, Geurts van Kessel A. 1995. Comparative genomic hybridization analysis of human sarcomas. II. Identification of novel amplicons at 6p and 17p in osteosarcomas. Genes Chromosomes Cancer 14:15–21.

Fujise K, Nagamori S, Hasumura S, Homma S, Sujino H, Matsuura T, Shimizu K, Niiya M, Kameda H, Fujita K. 1990. Integration of hepatitis B virus DNA into cells of six established human hepatocellular carcinoma cell lines. Hepatogastroenterology 37:457–460.

Garaude J, Cherni S, Kaminski S, Delepine E, Chable-Bessia C, Benkirane M, Borges J, Pandiella A, Iñiguez MA, Fresno M, Hipskind RA, Villalba M. 2006. ERK5 activates NF-kappaB in leukemic T cells and is essential for their growth in vivo. J Immunol 177:7607–7617.

Garraway LA, Widlund HR, Rubin MA, Getz G, Berger AJ, Ramaswamy S, Beroukhim R, Milner DA, Granter SR, Du J, Lee C, Wagner SN, Li C, Golub TR, Rimm DL, Meyerson ML, Fisher DE, Sellers WR. 2005. Integrative genomic analyses identify MITF as a lineage survival oncogene amplified in malignant melanoma. Nature 436:117–122.

Gírio A, Montero JC, Pandiella A, Chatterjee S. 2007. Erk5 is activated and acts as a survival factor in mitosis. Cell Signal 19:1964–1972.

Hayashi M, Lee JD. 2004. Role of the BMK1/ERK5 signaling pathway: Lessons from knockout mice. J Mol Med 82:800–808.

Hirohashi S, Shimosato Y, Kameya T, Koide T, Mukojima T, Taguchi Y, Kageyama K. 1979. Production of -fetoprotein and normal serum proteins by xenotransplanted human hepatomas in relation to their growth and morphology. Cancer Res 39: 1819–1828.

Huh N, Utakoji T. 1981. Production of HBs-antigen by two new human hepatoma cell lines and its enhancement by dexamethasone. Gann 72:178–179.

Kallioniemi A, Kallioniemi OP, Sudar D, Rutovitz D, Gray JW, Waldman F, Pinkel D. 1992. Comparative genomic hybridization for molecular cytogenetic analysis of solid tumors. Science 258:818–821.

Kato Y, Kravchenko VV, Tapping RI, Han J, Ulevitch RJ, Lee JD. 1997. BMK1/ERK5 regulates serum-induced early gene expression through transcription factor MEF2C. EMBO J 16:7054–7066.

Kato Y, Tapping RI, Huang S, Watson MH, Ulevitch RJ, Lee JD. 1998. Bmk1/Erk5 is required for cell proliferation induced by epidermal growth factor. Nature 395:713–716.

Kennedy GC, Matsuzaki H, Dong S, Liu WM, Huang J, Liu G, Su X, Cao M, Chen W, Zhang J, Liu W, Yang G, Di X, Ryder T, He Z, Surti U, Phillips MS, Boyce-Jacino MT, Fodor SP, Jones KW. 2003. Large-scale genotyping of complex DNA. Nat Biotechnol 21:1233–1237.

Knowles BB, Howe CC, Aden DP. 1980. Human hepatocellular carcinoma cell lines secrete the major plasma proteins and hepatitis B surface antigen. Science 209:497–499.

Linnerth NM, Baldwin M, Campbell C, Brown M, McGowan H, Moorehead RA. 2005. IGF-II induces CREB phosphorylation and cell survival in human lung cancer cells. Oncogene 24:7310–7319.

Little CD, Nau MM, Carney DN, Gazdar AF, Minna JD. 1983. Amplification and expression of the c-myc oncogene in human lung cancer cell lines. Nature 306:194–196.

Matsuzaki H, Dong S, Loi H, Di X, Liu G, Hubbell E, Law J, Berntsen T, Chadha M, Hui H, Yang G, Kennedy GC, Webster TA, Cawley S, Walsh PS, Jones KW, Fodor SP, Mei R. 2004a. Genotyping over 100,000 SNPs on a pair of oligonucleotide arrays. Nat Methods 1:109–111.

Matsuzaki H, Loi H, Dong S, Tsai YY, Fang J, Law J, Di X, Liu WM, Yang G, Liu G, Huang J, Kennedy GC, Ryder TB, Marcus GA, Walsh PS, Shriver MD, Puck JM, Jones KW, Mei R. 2004b. Parallel genotyping of over 10,000 SNPs using a one-primer assay on a high-density oligonucleotide array. Genome Res 14:414–425.

McCracken SR, Ramsay A, Heer R, Mathers ME, Jenkins BL, Edwards J, Robson CN, Marquez R, Cohen P, Leung HY. 2008. Aberrant expression of extracellular signal-regulated kinase 5 in human prostate cancer. Oncogene 27:2978–2988.

Mehta PB, Jenkins BL, McCarthy L, Thilak L, Robson CN, Neal DE, Leung HY. 2003. MEK5 overexpression is associated with metastatic prostate cancer, and stimulates proliferation, MMP-9 expression and invasion. Oncogene 22:1381–1389.

Mei R, Galipeau PC, Prass C, Berno A, Ghandour G, Patil N, Wolff RK, Chee MS, Reid BJ, Lockhart DJ. 2000. Genome-wide detection of allelic imbalance using human SNPs and high-density DNA arrays. Genome Res 10:1126–1137.

Minamiya Y, Matsuzaki I, Sageshima M, Saito H, Taguchi K, Nakagawa T, Ogawa J. 2004. Expression of tissue factor mRNA and invasion of blood vessels by tumor cells in non-small cell lung cancer. Surg Today 34:1–5.

Mulloy R, Salinas S, Philips A, Hipskind RA. 2003. Activation of cyclin D1 expression by the ERK5 cascade. Oncogene 22:5387–5398.

Nakabayashi H, Taketa K, Miyano K, Yamane T, Sato J. 1982. Growth of human hepatoma cells lines with differentiated functions in chemically defined medium. Cancer Res 42:3858–3863.

Nannya Y, Sanada M, Nakazaki K, Hosoya N, Wang L, Hangaishi A, Kurokawa M, Chiba S, Bailey DK, Kennedy GC, Ogawa S. 2005. A robust algorithm for copy number detection using high-density oligonucleotide single nucleotide polymorphism genotyping arrays. Cancer Res 65:6071–6079.

Nishimoto S, Nishida E. 2006. MAPK signalling: ERK5 versus ERK1/2. EMBO Rep 7:782–786.

Okamoto H, Yasui K, Zhao C, Arii S, Inazawa J. 2003. PTK2 and EIF3S3 genes may be amplification targets at 8q23–q24 and are associated with large hepatocellular carcinomas. Hepatology 38:1242–1249.

Park JG, Lee JH, Kang MS, Park KJ, Jeon YM, Lee HJ, Kwon HS, Park HS, Yeo KS, Lee KU, Kim ST, Chung JK, Hwang YJ, Lee HS, Kim GY, Lee YI, Chen TR, Hay RJ, Song SY, Kim WH, Kim CW, Kim YI. 1995. Characterization of cell lines established from human hepatocellular carcinoma. Int J Cancer 62:276–282.

Rosenthal JA, Chen H, Slepnev VI, Pellegrini L, Salcini AE, Di Fiore PP, De Camilli P. 1999. The epsins define a family of proteins that interact with components of the clathrin coat and contain a new protein module. J Biol Chem 274:33959–33965.

Sun W, Wei X, Kesavan K, Garrington TP, Fan R, Mei J, Anderson SM, Gelfand EW, Johnson GL. 2003. MEK kinase 2 and the adaptor protein Lad regulate extracellular signal-regulated kinase 5 activation by epidermal growth factor via Src. Mol Cell Biol 23:2298–2308.

Tarkkanen M, Karhu R, Kallioniemi A, Elomaa I, Kivioja AH, Nevalainen J, Böhling T, Karaharju E, Hyytinen E, Knuutila S, Kallioniemi OP. 1995. Gains and losses of DNA sequences in osteosarcomas by comparative genomic hybridization. Cancer Res 55:1334–1338.

van Dartel M, Cornelissen PW, Redeker S, Tarkkanen M, Knuutila S, Hogendoorn PC, Westerveld A, Gomes I, Bras J, Hulsebos TJ. 2002. Amplification of 17p11.2 approximately p12, including PMP22, TOP3A, and MAPK7, in high-grade osteosarcoma. Cancer Genet Cytogenet 139:91–96.

Wang X, Tournier C. 2006. Regulation of cellular functions by the ERK5 signalling pathway. Cell Signal 18:753–760.

Weldon CB, Scandurro AB, Rolfe KW, Clayton JL, Elliott S, Butler NN, Melnik LI, Alam J, McLachlan JA, Jaffe BM, Beckman BS, Burow ME. 2002. Identification of mitogen-activated protein kinase kinase as a chemoresistant pathway in MCF-7 cells by using gene expression microarray. Surgery 132:293–301.

Wong KK, Tsang YT, Shen J, Cheng RS, Chang YM, Man TK, Lau CC. 2004. Allelic imbalance analysis by high-density single-nucleotide polymorphic allele (SNP) array with whole genome amplified DNA. Nucleic Acids Res 32:e69.

Yasui K, Arii S, Zhao C, Imoto I, Ueda M, Nagai H, Emi M, Inazawa J. 2002. TFDP1, CUL4A, and CDC16 identified as targets for amplification at 13q34 in hepatocellular carcinomas. Hepatology 35:1476–1484.

Yasui K, Imoto I, Fukuda Y, Pimkhaokham A, Yang ZQ, Naruto T, Shimada Y, Nakamura Y, Inazawa J. 2001. Identification of target genes within an amplicon at 14q12-q13 in esophageal squamous cell carcinoma. Genes Chromosomes Cancer 32:112–118.

Yokoi S, Yasui K, Iizasa T, Imoto I, Fujisawa T, Inazawa J. 2003. TERC identified as a probable target within the 3q26 amplicon that is detected frequently in non-small cell lung cancers. Clin Cancer Res 9:4705–4713.

Yokoi S, Yasui K, Saito-Ohara F, Koshikawa K, Iizasa T, Fujisawa T, Terasaki T, Horii A, Takahashi T, Hirohashi S, Inazawa J. 2002. A novel target gene, SKP2, within the 5p13 amplicon that is frequently detected in small cell lung cancers. Am J Pathol 161:207–216.

Yuste L, Montero JC, Esparis-Ogando A, Pandiella A. 2005. Activation of ErbB2 by overexpression or by transmembrane neuregulin results in differential signaling and sensitivity to herceptin. Cancer Res 65:6801–6810.

Zhao X, Li C, Paez JG, Chin K, Jänne PA, Chen TH, Girard L, Minna J, Christiani D, Leo C, Gray JW, Sellers WR, Meyerson M. 2004. An integrated view of copy number and allelic alterations in the cancer genome using single nucleotide polymorphism arrays. Cancer Res 64:3060–3071.

Zhao X, Weir BA, LaFramboise T, Lin M, Beroukhim R, Garraway L, Beheshti J, Lee JC, Naoki K, Richards WG, Sugarbaker D, Chen F, Rubin MA, Jänne PA, Girard L, Minna J, Christiani D, Li C, Sellers WR, Meyerson M. 2005. Homozygous deletions and chromosome amplifications in human lung carcinomas revealed by single nucleotide polymorphism array analysis. Cancer Res 65:5561–5570.